

Black Holes in the Red-sequence Elliptical Galaxies at Redshifts $\sim 0.7 - 2.5$: Not Dark Energy Source but Remnants of Little Red Dots

Lei Lei,^{1,2} Ze-Fan Wang,^{1,2} Yi-Ying Wang,^{1,2} Lei Feng,^{1,2,*} and Yi-Zhong Fan^{1,2,†}

¹Key Laboratory of Dark Matter and Space Astronomy,

Purple Mountain Observatory, Chinese Academy of Sciences, Nanjing 210033, China

²School of Astronomy and Space Science, University of Science and Technology of China, Hefei, Anhui 230026, China

(Dated: June 25, 2025)

The nature of dark energy remains one of the most profound mysteries in modern cosmology. One intriguing proposal is that black holes (BHs) could be the astrophysical source of dark energy through a cosmological coupling mechanism, and strong evidence has been claimed via analyzing the growth of the black hole masses in the red-sequence elliptical galaxies at redshifts ≤ 2.5 . In this work, with a group of very high redshift AGNs detected by the James Webb Space Telescope (JWST) in the red-sequence elliptical galaxies, we show that the possibility of BHs being the astrophysical source of dark energy has been rejected at a confidence level exceeding 10σ . Moreover, it turns out that the Little Red Dots recently discovered by JWST, characterized by the low accretion rates, can naturally evolve into the red-sequence elliptical galaxies hosting the relatively low mass black holes at the redshifts of $\sim 0.7 - 2.5$, without the need of black hole cosmological coupling.

Introduction— Dark energy is believed to be the driving force behind the accelerated expansion of the universe [1, 2], but its nature remains elusive [3, 4]. Various models have been proposed to account for the dark energy, including the cosmological constant [1, 2], the scalar field [5, 6], quintessence [7, 8], phantom [9], quintom [10, 11], modified gravity [12], coupled dark energy scenarios [13, 14], and so on.

A recent intriguing idea is that black holes, particularly stellar remnant black holes (BHs), could be the astrophysical origin of dark energy through a cosmological coupling mechanism [15–17]. This mechanism can be realized through non-singular black holes embedding with the cosmological background [18–22] (see, however, Ref. [23–26]). According to this hypothesis, the mass of BHs would grow with the cosmic scale factor a as $M_{\text{BH}}(a) = M_{\text{BH}}(a_i) \times \left(\frac{a}{a_i}\right)^k$, where k is the cosmological coupling strength [17]. If $k \sim 3$, the BHs contribute as a cosmological dark energy species. The strength $k = 0$, instead, represents the absence of coupling between black holes and the accelerated expansion of the universe. A preferential growth channel for supermassive black holes in red-sequence elliptical galaxies found by Farrah et al. [16] gave strong cosmological coupling evidence with a strength $k = 3.09 \pm 0.76$ [17]. Moreover, the astrophysical black holes produced during the process of star formation can meet the cosmological dark energy density proportion of $\Omega_\Lambda = 0.68$ through cosmological coupling, without violating the existing limits of the abundance of the massive compact halo objects (MACHOs) [17].

As the astrophysical origin of dark energy, cosmologically coupled black holes may play some key roles. For instance, the cosmologically coupled mass growth of black holes can solve the low mass gap problem [27] and provide a potential candidate for the time-evolving dark energy source that naturally explains the recent baryon acoustic oscillation (BAO) measurements by the Dark Energy Spectroscopic Instrument

(DESI) [28]. The cosmologically coupled BHs can fit well with BAO data with a peaked positive summed neutrino mass $\Sigma m_\nu = 0.106$, which is in good agreement with lower limits from neutrino oscillation experiments [29]. These objects can provide anisotropic dark energy [30] that has also received widespread attention [31, 32].

Dedicated tests have been carried out but the conclusions are controversial. In some works, the cosmological coupling is favored. For instance, Cadoni et al. [33] reached the same conclusion as Ref. [16] based on similar data. The gravitational-wave background (GWB) from SMBHs measured by pulsar timing arrays favors the strong coupling strength $k \approx 3$ [34]. A strong coupling strength $k > 2$ is preferred by comparing the GWB spectral index of SMBH mergers and the current GWB measurements [35]. While in some other works, the cosmological coupling is not supported. For example, Andrae and El-Badry [36] found that the probability of the non-cosmological coupling was 77% from Gaia observations. The high-redshift AGNs observed by JWST tend to suggest the absence of cosmological coupling [37]. The minimal formation mass of the BHs in the GWTC-3 gravitational wave observations disfavors the cosmological coupling model at 2σ level [38]. A non-coupling BH population is favored with stellar-mass BHs in X-ray binaries using their masses and ages [39]. The strongest constraint comes from the study with the mass function of black holes in the globular cluster NGC 3201, for which there was only a probability of 10^{-4} for the BHs' cosmological coupling [40], i.e., such a possibility is disfavored at a confidence level of 3.8σ . Anyhow, a decisive constraint at a confidence level above 5σ is still lacking.

In this work, different from the previous approach with a rather limited host mass range [37], we take the significantly increased sample of very high-redshift AGNs and quasars detected by the JWST to assess the viability of BHs as the source of dark energy by the cosmological coupling. The cosmological parameters used in this work include $H_0 = 67.36 \text{ km s}^{-1} \text{ Mpc}^{-1}$, $\Omega_m = 0.3135$ and $\Omega_\Lambda = 0.6847$ [41]. Our main finding is that such a possibility has been rejected at a confidence level of $\sim 11\sigma$. We also show that the little

* fenglei@pmo.ac.cn

† yzf@pmo.ac.cn

red dots (LRDs) recently discovered by JWST can naturally evolve into the red-sequence elliptical galaxies at the redshifts of $\sim 0.7 - 2.5$, which further weakens the black hole dark energy hypothesis.

Data— JWST is well suitable to measure high redshift objects, and these data have been widely adopted to test the models of dark energy or dark matter [42–46].

The high-resolution spectra of JWST have been widely adopted to search for AGNs, as their significant broad emission line features can be used to calculate black hole mass [47–49]. The JWST’s highly sensitive photometric camera can also provide high quality images to separate the host galaxies of AGNs [50, 51].

The mass of black holes coupled with cosmology will evolve significantly with redshift. In this theory, the mass of black holes in AGNs will show noticeable growth independent of the host galaxy over time, while the stellar mass of red-sequence elliptical galaxies will not change much during evolution [15, 17]. Therefore, to examine the mass growth patterns caused by the cosmological coupling of black holes in AGNs, we select samples of sufficiently old host galaxies [16]. The red-sequence elliptical galaxies can ensure that the mass of the host galaxies remains relatively constant during prolonged evolution [16, 37]. The higher the redshift, the more pronounced the redshift evolution of supermassive black hole mass relative to the mass of the host galaxy, but high-redshift red-sequence elliptical host galaxy AGN samples are very rare.

Due to sample size limitations, previous work using JWST’s AGN samples to test cosmologically coupled black holes only filtered sources meeting certain conditions [37]. As shown in Refs. [50, 52, 53], the low-luminosity group of AGN observed by JWST has a significantly higher black hole mass-to-stellar mass ratio than the high-luminosity group. These low stellar mass samples may introduce biases when testing the cosmological coupled black hole theory [37]. Therefore, in this work, we select the bright, high stellar mass quasars observed by JWST to avoid biases from the low luminosity population.

Among the numerous AGNs observed by JWST, more than 10 host galaxy stellar masses exceed 4×10^{10} solar masses [47–50, 54], making these samples suitable for testing cosmological coupled black hole theories.

To avoid the effects of accretion growth of black holes, star formation, and other factors on the redshift evolution of the relationship between supermassive black hole mass and host galaxy stellar mass, the selected sample meets the following conditions [16, 17, 37]:

- Redshift: We select the AGNs at high redshift $z > 2.0$. As listed in Table I, we selected the sample in a range of $2.0 < z < 7$.
- Dust Extinction: We select the blue AGNs with $E(B - V) < 0.5$.
- Host type: Following Farrah et al. [16, 17], we select the red-sequence elliptical host galaxies without structures like shells, spiral arms or disks in their images.

- Stellar mass (M_\star): Same as Farrah et al. [16, 17], we select the sample with host stellar masses higher than $4 \times 10^{10} M_\odot$.
- Star Formation Rate (SFR): Following Lei et al. [37], we select the AGN host galaxies that are below the SFR – M_\star main sequence relationship ψ_{SFR} and the intrinsic scatter δ_{SFR} at the redshift of the source.

The SFR – M_\star main sequence relationship at $z \sim 0 - 6$ is adopted from Speagle et al. [55], while for the redshift range of $z \sim 6 - 10$ we use the relationship suggested by the JWST data [56]. The SFRs of AGN host galaxies are estimated using H α narrow emission line.

The sample with low-dust extinction $E(B - V) < 0.5$ is selected as blue quasars. We adopt a conversion factor of dust extinction $A_V/E(B - V) = 4.05$ [53]. In Harikane et al. [53], the extinction threshold for the high-redshift ($z > 4$) red AGN sample is taken to be $E(B - V) = 0.5$. We also calculated the distribution of extinction of the JWST red AGN sample in Labbe et al. [60] and confirmed such a threshold.

Our AGN sample of red-sequence elliptical host galaxies is summarized in Table I. The black hole mass and the stellar mass of the host galaxies of our selected sample are shown in Figure 1, which are consistent with the samples of the local universe.

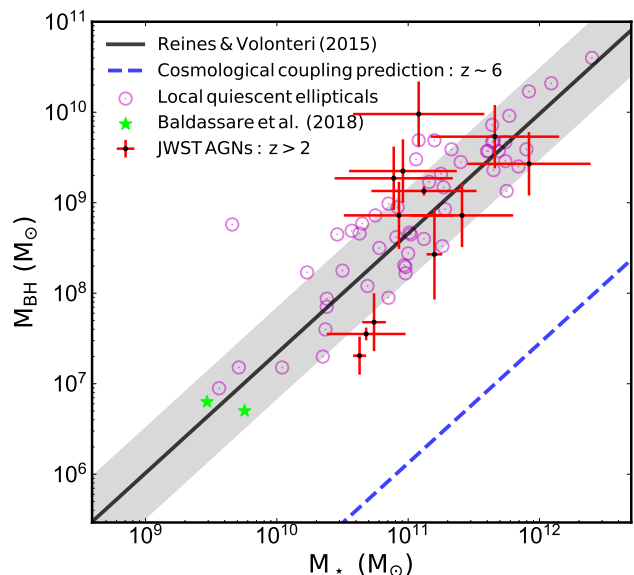


FIG. 1. Our selected AGNs and the local sample. The black line shows the $M_\star - M_{\text{BH}}$ fundamental plane relationship of local elliptical host AGNs. The data points with error bars are the 12 selected AGNs in this work from Refs. [47–51, 54, 57–59]. The circles in purple are local quiescent elliptical AGNs from Farrah et al. [16]. The green stars are two local AGNs in dwarf ETGs taken from Ben-Ami et al. [61]. The blue dashed line represents the predicted relationship when the cosmological coupling strength is set to $k = 3$.

Methods— The $M_\star - M_{\text{BH}}$ fundamental plane is a well-established empirical relationship [62–64]. It is based on the observation that the mass of a supermassive black hole at the

TABLE I. The selected JWST AGN sample in this work.

ID	redshift	E(B-V)	SFR (M_{\odot}/yr)	$\log_{10}(M_{\star}/M_{\odot})$	$\log_{10}(M_{\text{BH}}/M_{\odot})$	Reference
GN-9994014	5.32	$< 0.5^{\text{a}}$	13.2 ± 3.2	10.68 ± 0.30	7.55 ± 0.07	[48]
GS-204851	5.48	0.02	$21.4 \pm 8.1^{\text{b}}$	10.74 ± 0.09	7.68 ± 0.32	[49, 57]
J2236+0032	6.40	0.28	$< 100^{\text{c,f}}$	11.12 ± 0.40	9.13 ± 0.05	[47]
J0148+0600	5.98	0.35	$299.6 \pm 74.9^{\text{c,d}}$	11.08 ± 0.50	9.98 ± 0.36	[50, 51]
J1030+0524	6.30	0.49	$543.8 \pm 130.2^{\text{c,d}}$	10.89 ± 0.45	9.27 ± 0.35	[50, 51]
J1148+5251	6.42	0.36	$311.1 \pm 77.7^{\text{c,d}}$	11.66 ± 0.49	9.73 ± 0.35	[50, 51]
J0218+0007	6.77	0.44	$1.0 \pm 0.3^{\text{c,d}}$	11.41 ± 0.39	8.86 ± 0.35	[50, 58]
J0224-4711	6.52	0.44	$10.7 \pm 2.3^{\text{c,e}}$	11.92 ± 0.47	9.43 ± 0.35	[50, 58]
J0305-3150	6.61	0.43	$< 100^{\text{c,e,f}}$	10.93 ± 0.42	8.86 ± 0.37	[50, 58]
J2232+2930	6.67	0.33	$12.2 \pm 3.1^{\text{c,e}}$	10.96 ± 0.41	9.35 ± 0.35	[50, 58]
COS-XQG1	2.09	0.21	1.5 ± 0.2	11.20 ± 0.06	8.43 ± 0.50	[59]
GN-72127	4.13	0.11	0.1 ± 0.8	10.63 ± 0.05	7.31 ± 0.21	[54]

^a Zhang et al. [48] did not provide an exact extinction value. We estimate this upper limit with the UV slope given by Zhang et al. [48]. As shown in Figure 15 of Ref. [50], the dust extinction of AGN is $A_V < 2.0$ for the sources with UV slopes $\beta_{\text{UV}} < 1.35$.

^b The SFR is estimated with the luminosity of the narrow $\text{H}\alpha$ line fitted in Ref. [57].

^c The SFR values are estimated with the luminosity of the narrow $\text{H}\alpha$ line. The narrow $\text{H}\alpha$ line luminosity is converted from the narrow $\text{H}\beta$ line luminosity by a factor $L_{\text{H}\alpha, \text{broad}}/L_{\text{H}\alpha, \text{narrow}} = 3.05$ (a statistical result of $z > 5$ AGNs [49]).

^d The luminosity of narrow $\text{H}\beta$ line is fitted by the Gaussian profile model in Ref. [51].

^e The luminosity of narrow $\text{H}\beta$ line is fitted by the Gaussian profile model in Ref. [58].

^f There is no significant narrow line was found. Thus we estimated an upper limit of SFR.

centre of a galaxy is correlated with the stellar mass of its host galaxy. For the AGNs in the red-sequence elliptical host galaxies, we have [37]

$$\log_{10}\left(\frac{M_{\text{BH}}}{M_{\odot}}\right) = 8.66_{-0.01-0.5}^{+0.01+0.5} + 1.32_{-0.01}^{+0.01} \times \log_{10}\left(\frac{M_{\star}}{10^{11} M_{\odot}}\right), \quad (1)$$

where M_{BH} is the black hole mass and M_{\star} is the stellar mass of the host galaxy. The errors are the 1σ standard deviations found in the fitting, and the 0.5 dex refers to the intrinsic scatter of the local sample shown in the grey region in Figure 1. This relationship has been adopted to compare the high-redshift AGNs with local samples. If there is a cosmological coupling between BHs and dark energy, we would expect the intercept of this relationship to evolve with redshift. Given that our sample consists of host galaxies with $M_{\star} > 4 \times 10^{10} M_{\odot}$, the impact of observational biases is relatively small.

To estimate the parameter k , we have the relationship of

$$\mu_i(k) = 1.32 \times \log_{10}\left(\frac{M_{\star,i}}{M_{\odot}}\right) - k \times \log_{10}(1 + z_i) - 5.86, \quad (2)$$

which likelihood reads [37]

$$\mathcal{L}(d|k) = \prod_i \frac{1}{\sigma_i \sqrt{2\pi}} \exp\left\{-\frac{[\mu_i(k) - \log_{10}\left(\frac{M_{\text{BH},i}}{M_{\odot}}\right)]^2}{2(\sigma_i)^2}\right\}, \quad (3)$$

where $M_{\text{BH},i}$ and σ_i are the observed BH mass and the error including the uncertainties of $M_{\text{BH},i}$ and $M_{\star,i}$, respectively. The total error includes measured BH mass error ($\sigma_{\text{BH},i}$), conversion error ($\sigma_{\text{conv},i}$) from stellar mass and fundamental plane intrinsic scatter $\sigma_{\text{intrinsic}} = 0.5$ dex [37]

$$\sigma_{\text{tot},i}^2 = \sigma_{\text{BH},i}^2 + \sigma_{\text{conv},i}^2 + \sigma_{\text{intrinsic}}^2. \quad (4)$$

The errors in our data are in the logarithmic space. Here, z_i denotes the cosmological redshift of the source.

Using the fundamental relationship between the stellar mass of quasars and the black hole mass filtered from Table I of the host galaxies, we can estimate the value of the cosmological coupling strength k using the Markov Chain Monte Carlo method.

Result and discussion— Our analysis reveals that the high-redshift AGN sample has BH masses that are significantly higher than those predicted by the cosmological coupling growth theory with $k = 3$. Indeed, the best-fit value of the coupling strength parameter k is found to be

$$k = 0.13 \pm 0.27 \text{ (68\% confidence interval)}, \quad (5)$$

which deviates from the value of $k = 3$ required for BHs to serve as dark energy at a confidence level of $\approx 11\sigma$. Instead, it is remarkably consistent with the prediction of the non-cosmologically coupled black holes ($k = 0$).

We conclude that the JWST high-redshift AGNs have convincingly ruled out the possibility of BHs being the source of dark energy. As shown below, these objects are likely the descendants of the little red dots, a specific group of AGNs in the high-redshift universe, recently discovered by JWST [60, 65]. Compared to bright AGNs, the LRDs are characterized by their redder colors, lower masses, and lower accretion rates [50, 66]. The $M_{\text{BH}} - M_{\star}$ distribution of the LRDs are shown as the black points with error bars in Figure 3.

LRDs may have strong star formation potential [57], but their black hole accretion growth rate is very slow [50, 66], and the peak in the number density redshift distribution of this group of targets is at the redshift range of 5–8 [67, 68], which is significantly different from the peak in the density distribution of ordinary bright AGNs (at redshift of 1–3, Ma et al. [67]). As shown below, this provides a viable explanation for

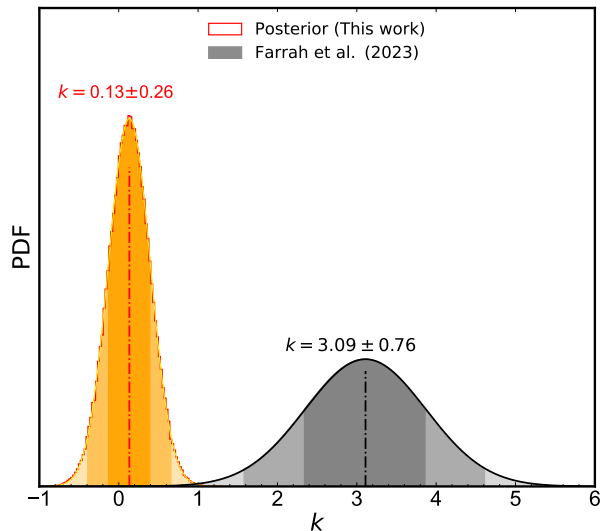


FIG. 2. Probability distribution function of the posterior of the cosmological coupling strength parameter k . The orange distribution is our result inferred from the very high redshift AGNs detected by JWST, which is significantly different from that found in Ref. [17] and rules out the cosmological coupling model.

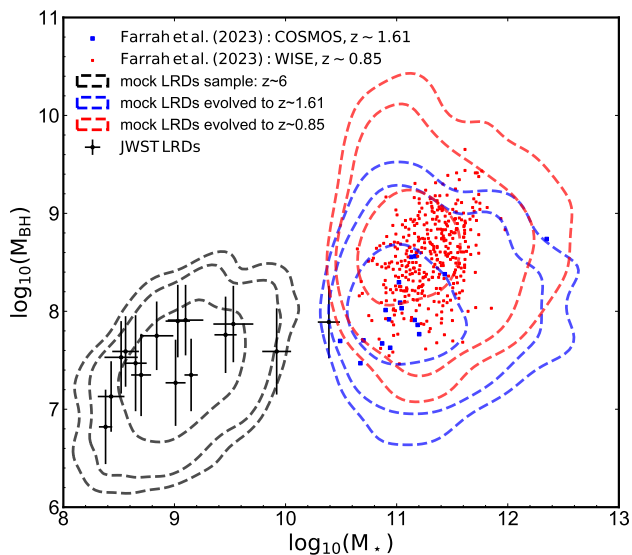


FIG. 3. The evolution history of the JWST little red dots is consistent with the evolution of the sample of AGNs with red-sequence elliptical hosts. The selected $z \sim 0.85$ and $z \sim 1.61$ AGNs from Ref. [17] are shown as red and blue points. The dashed contours in black, blue and red show our simulated LRDs redshift $z \sim 6$, $z \sim 1.61$ and $z \sim 0.85$. Three contours correspond to sample density levels of 0.05, 0.1, and 0.3, respectively. The black points with error bars are JWST LRDs adopted from Ref. [50].

the evolution of the specific black hole population reported in Ref. [17].

To explore whether LRDs could provide a natural astrophysical explanation for the sample used in Ref. [17], we con-

ducted simulations of LRD evolution in the $M_{\text{BH}} - M_{\star}$ plane, as illustrated in Figure 3. Using the sample of LRDs observed by JWST at $z \approx 6$ [50], we generated 1000 mock sources whose stellar masses and black hole masses follow a two-dimensional log-normal distribution consistent with the observed properties of this population. We adopted the following initial conditions based on JWST observations:

- Initial stellar masses are distributed as $\log_{10}(M_{\star}/M_{\odot}) = 9.05 \pm 0.4$ and black hole masses as $\log_{10}(M_{\text{BH}}/M_{\odot}) = 7.35 \pm 0.5$, matching the observed LRD population [50].
- Star formation rates follow a relationship with stellar mass that is consistent with measurements of JWST LRDs: $\log_{10}(\text{SFR}/(M_{\odot}/\text{yr})) = 0.7 \times \log_{10}(M_{\star}/M_{\odot}) - 5.3$ with log-normal scatter of 0.8 dex [50, 55].
- Black hole accretion rates are assigned using the relation $\log_{10}(\dot{M}_{\text{BH}}/(M_{\odot}/\text{yr})) = \log_{10}(M_{\text{BH}}/M_{\odot}) - 9.0$ with log-normal scatter of 0.5 dex, consistent with observations [50, 69].

We then computed the growth of stellar masses and black hole masses from $z \sim 6$ to $z \sim 1.61$, assuming constant SFR values and constant black hole accretion rates during this epoch. Given that the host galaxies of the COSMOS-selected sample studied in Ref. [17] are already red-sequence elliptical systems at $z \sim 1.61$, we assume that the host galaxies of LRDs that evolve into these systems have effectively quenched their star formation. However, we maintain their black hole accretion rates at approximately constant values, consistent with their initially low accretion rates.

During the subsequent evolutionary phase from $z \sim 1.61$ to $z \sim 0.85$, we therefore set the SFR values of the simulated sample as $\text{SFR} = 0 M_{\odot} \text{yr}^{-1}$ with log-normal scatter of 0.8 dex (the conclusion is unchanged if we still take the initial non-zero star formation rate), while maintaining the black hole accretion rates at their previous levels.

After completing these evolutionary calculations, we selected mock sources with the host galaxy stellar masses satisfying $M_{\star} > 4 \times 10^{10} M_{\odot}$, matching the selection criteria of Ref. [17]. The resulting distributions are plotted in Figure 3 as dashed contours. Remarkably, the evolutionary trajectories of LRDs produce distributions that closely match the properties of the red-sequence elliptical galaxies [17].

As evident in Figure 3, when evolved to $z \sim 1.61$ (blue contour), our simulated sources show excellent agreement with the COSMOS AGN sample at the same redshift (blue points). Assuming that these sources continue to evolve with quenched star formation but sustained low-level black hole accretion, they naturally progress to the distribution shown by the red contour at $z \sim 0.85$, which closely corresponds to the observed WISE sample at this redshift (red points).

Our simulation demonstrates that the little red dots currently observed by JWST can naturally explain the black holes in the red-sequence elliptical galaxies at redshifts of 0.7 – 2.5 [17], without the need to introduce black hole cosmological coupling, which provides an additional support to our conclusion made at the beginning of this section.

Future observations with the JWST and other advanced telescopes, such as the China Space Station Telescope (CSST), Euclid and the ROMAN space telescope, will provide more detailed information on the coevolution of AGN and their host galaxies, further promoting our understanding of the growth of the supermassive black holes.

ACKNOWLEDGMENTS

We thank Lei Zu, Guan-Wen Yuan, Zhen-Bo Su, Wen-Ke Ren, Chi Zhang, and Da-Ming Wei for helpful dis-

cussions. The authors were supported in part by the National Key Research and Development Program of China (No. 2022YFF0503301) and by NSFC under grants of No.12233011 and No.12373002.

-
- [1] A. G. Riess, A. V. Filippenko, P. Challis, A. Clocchiatti, A. Diercks, P. M. Garnavich, R. L. Gilliland, C. J. Hogan, S. Jha, R. P. Kirshner, et al., *Astron. J.* **116**, 1009 (1998), astro-ph/9805201.
- [2] S. Perlmutter, G. Aldering, G. Goldhaber, R. A. Knop, P. Nugent, P. G. Castro, S. Deustua, S. Fabbro, A. Goobar, D. E. Groom, et al., *Astrophys. J.* **517**, 565 (1999), astro-ph/9812133.
- [3] J. Frieman, M. Turner, and D. Huterer, *Ann. Rev. Astron. Astrophys.* **46**, 385 (2008), 0803.0982.
- [4] M. Li, X.-D. Li, S. Wang, and Y. Wang, *Commun. Theor. Phys.* **56**, 525 (2011), 1103.5870.
- [5] R. R. Caldwell, R. Dave, and P. J. Steinhardt, *Phys. Rev. Lett.* **80**, 1582 (1998), astro-ph/9708069.
- [6] P. G. Ferreira and M. Joyce, *Phys. Rev. D* **58**, 023503 (1998), astro-ph/9711102.
- [7] R. R. Caldwell and E. V. Linder, *Phys. Rev. Lett.* **95**, 141301 (2005), astro-ph/0505494.
- [8] S. Tsujikawa, *Class. Quant. Grav.* **30**, 214003 (2013), 1304.1961.
- [9] R. R. Caldwell, M. Kamionkowski, and N. N. Weinberg, *Phys. Rev. Lett.* **91**, 071301 (2003), astro-ph/0302506.
- [10] Y.-F. Cai, E. N. Saridakis, M. R. Setare, and J.-Q. Xia, *Phys. Rept.* **493**, 1 (2010), 0909.2776.
- [11] T. Qiu, *Modern Physics Letters A* **25**, 909 (2010), 1002.3971.
- [12] Y.-F. Cai, S. Capozziello, M. De Laurentis, and E. N. Saridakis, *Rept. Prog. Phys.* **79**, 106901 (2016), 1511.07586.
- [13] L. Amendola, C. Quercellini, D. Tocchini-Valentini, and A. Pasqui, *Astrophys. J. Lett.* **583**, L53 (2003), astro-ph/0205097.
- [14] L. Amendola and C. Quercellini, *Phys. Rev. D* **68**, 023514 (2003), astro-ph/0303228.
- [15] K. S. Croker, K. A. Nishimura, and D. Farrah, *Astrophys. J.* **889**, 115 (2020), 1904.03781.
- [16] D. Farrah, S. Petty, K. S. Croker, G. Tarlé, M. Zevin, E. Hatziminaoglou, F. Shankar, L. Wang, D. L. Clements, A. Efsthathiou, et al., *Astrophys. J.* **943**, 133 (2023), 2212.06854.
- [17] D. Farrah et al., *Astrophys. J. Lett.* **944**, L31 (2023), 2302.07878.
- [18] V. Faraoni and M. Rinaldi, *Phys. Rev. D* **110**, 063553 (2024), 2407.14549.
- [19] M. Cadoni, R. Murgia, M. Pitzalis, and A. P. Sanna, *JCAP* **03**, 026 (2024), 2309.16444.
- [20] V. Faraoni and C. Zeyn, *Phys. Rev. D* **109**, 124002 (2024), 2401.00091.
- [21] M. Cadoni, M. Pitzalis, and A. P. Sanna, *JCAP* **02**, 051 (2025), 2410.10459.
- [22] M. Almatwi, *Eur. Phys. J. C* **84**, 845 (2024), 2408.13559.
- [23] P. P. Avelino, *JCAP* **08**, 005 (2023), 2303.06630.
- [24] T. Mistele, *Res. Notes AAS* **7**, 101 (2023), 2304.09817.
- [25] R. Gaur and M. Visser, *Phys. Rev. D* **110**, 043529 (2024), 2308.07374.
- [26] P. K. Dahal, S. Maharana, F. Simovic, I. Soranidis, and D. R. Terno, *Phys. Rev. D* **110**, 044032 (2024), 2312.16804.
- [27] S.-J. Gao and X.-D. Li, *Astrophys. J.* **956**, 128 (2023), 2307.10708.
- [28] K. S. Croker, G. Tarlé, S. P. Ahlen, B. G. Cartwright, D. Farrah, N. Fernandez, and R. A. Windhorst, *JCAP* **10**, 094 (2024), 2405.12282.
- [29] S. Ahlen, A. Aviles, B. Cartwright, K. S. Croker, W. Elbers, D. Farrah, N. Fernandez, G. Niz, J. Rohlf, G. Tarlé, et al., arXiv e-prints arXiv:2504.20338 (2025), 2504.20338.
- [30] R. Chan, M. F. A. da Silva, and P. Rocha, *Gen. Rel. Grav.* **43**, 2223 (2011), 1009.4403.
- [31] R. Zhang and Z. Zhang, *JCAP* **06**, 031 (2023), 2303.14047.
- [32] R. Mc Conville and E. O. Colgáin, *Phys. Rev. D* **108**, 123533 (2023), 2304.02718.
- [33] M. Cadoni, A. P. Sanna, M. Pitzalis, B. Banerjee, R. Murgia, N. Hazra, and M. Branchesi, *JCAP* **11**, 007 (2023), 2306.11588.
- [34] M. Lacy, A. Engholm, D. Farrah, and K. Ejercito, *Astrophys. J. Lett.* **961**, L33 (2024), 2312.12344.
- [35] M. Calzà, F. Gianesello, M. Rinaldi, and S. Vagnozzi, *Sci. Rep.* **14**, 31296 (2024), 2409.01801.
- [36] R. Andrae and K. El-Badry, *Astron. Astrophys.* **673**, L10 (2023), 2305.01307.
- [37] L. Lei et al., *Sci. China Phys. Mech. Astron.* **67**, 229811 (2024), 2305.03408.
- [38] L. Amendola, D. C. Rodrigues, S. Kumar, and M. Quartin, *Mon. Not. Roy. Astron. Soc.* **528**, 2377 (2024), 2307.02474.
- [39] E. Mlinar and T. Zwitter, *Mon. Not. Roy. Astron. Soc.* **528**, 3000 (2024), 2311.09007.
- [40] C. L. Rodriguez, *Astrophys. J. Lett.* **947**, L12 (2023), 2302.12386.
- [41] Planck Collaboration, N. Aghanim, Y. Akrami, M. Ashdown, J. Aumont, C. Baccigalupi, M. Ballardini, A. J. Banday, R. B. Barreiro, N. Bartolo, et al., *Astron. Astrophys.* **641**, A6 (2020), 1807.06209.
- [42] Y.-Y. Wang, L. Lei, G.-W. Yuan, and Y.-Z. Fan, *Astrophys. J. Lett.* **954**, L48 (2023), 2307.12487.
- [43] R. Janish and E. Pinetti, *Phys. Rev. Lett.* **134**, 071002 (2025), 2310.15395.
- [44] S. Roy, C. Blanco, C. Dessert, A. Prabhu, and T. Temim, *Phys. Rev. Lett.* **134**, 071003 (2025), 2311.04987.

- [45] L. Lei, Y.-Y. Wang, G.-W. Yuan, T.-L. Wang, M. A. T. Groenewegen, and Y.-Z. Fan, *Astrophys. J.* **980**, 249 (2025), 2501.07119.
- [46] Z.-F. Wang, L. Lei, L. Feng, and Y.-Z. Fan, *Res. Astron. Astrophys.* **24**, 125012 (2024), 2411.08774.
- [47] X. Ding, M. Onoue, J. D. Silverman, Y. Matsuoka, T. Izumi, M. A. Strauss, K. Jahnke, C. L. Phillips, J. Li, M. Volonteri, et al., *Nature (London)* **621**, 51 (2023), 2211.14329.
- [48] J. Zhang, E. Egami, F. Sun, X. Lin, J. Lyu, Y. Zhu, P. Rinaldi, Y. Sun, A. J. Bunker, R. Bhatawdekar, et al., arXiv e-prints arXiv:2505.02895 (2025), 2505.02895.
- [49] I. Juodžbalis, R. Maiolino, W. M. Baker, E. C. Lake, J. Scholtz, F. D'Eugenio, B. Trefoloni, Y. Isobe, S. Tacchella, A. J. Bunker, et al., arXiv e-prints arXiv:2504.03551 (2025), 2504.03551.
- [50] R. Li, L. C. Ho, and C.-H. Chen, arXiv e-prints arXiv:2505.12867 (2025), 2505.12867.
- [51] M. Yue, A.-C. Eilers, R. A. Simcoe, R. Mackenzie, J. Matthee, D. Kashino, R. Bordoloi, S. J. Lilly, and R. P. Naidu, *Astrophys. J.* **966**, 176 (2024), 2309.04614.
- [52] R. Maiolino et al., *Astron. Astrophys.* **691**, A145 (2024), 2308.01230.
- [53] Y. Harikane, Y. Zhang, K. Nakajima, M. Ouchi, Y. Isobe, Y. Ono, S. Hatano, Y. Xu, and H. Umeda, *Astrophys. J.* **959**, 39 (2023), 2303.11946.
- [54] V. Kokorev, J. Chisholm, R. Endsley, S. L. Finkelstein, J. E. Greene, H. B. Akins, V. Bromm, C. M. Casey, S. Fujimoto, I. Labbé, et al., *Astrophys. J.* **975**, 178 (2024), 2407.20320.
- [55] J. S. Speagle, C. L. Steinhardt, P. L. Capak, and J. D. Silverman, *Astrophys. J. Suppl.* **214**, 15 (2014), 1405.2041.
- [56] K. E. Heintz et al., *Nature Astron.* **7**, 1517 (2023), 2212.02890.
- [57] J. Matthee et al., *Astrophys. J.* **963**, 129 (2024), 2306.05448.
- [58] J. Yang et al., *Astrophys. J. Lett.* **951**, L5 (2023), 2304.09888.
- [59] K. Ito, T. S. Tanaka, K. Shimasaku, M. Ando, M. Onoue, M. Tanaka, S. Matsui, T. Kakimoto, and F. Valentino, *Monthly Notices of the Royal Astronomical Society* **538**, 1501 (2025), ISSN 0035-8711, <https://academic.oup.com/mnras/article-pdf/538/3/1501/62245817/staf372.pdf>, URL <https://doi.org/10.1093/mnras/staf372>.
- [60] I. Labbe, J. E. Greene, R. Bezanson, S. Fujimoto, L. J. Furtak, A. D. Goulding, J. Matthee, R. P. Naidu, P. A. Oesch, H. Atek, et al., *Astrophys. J.* **978**, 92 (2025), 2306.07320.
- [61] S. Ben-Ami, A. Vikhlinin, and A. Loeb, *Astrophys. J.* **854**, 4 (2018), 1712.03207.
- [62] J. Kormendy and L. C. Ho, *Ann. Rev. Astron. Astrophys.* **51**, 511 (2013), 1304.7762.
- [63] A. E. Reines and M. Volonteri, *Astrophys. J.* **813**, 82 (2015), 1508.06274.
- [64] M.-Y. Zhuang and L. C. Ho, *Nature Astronomy* **7**, 1376 (2023), 2308.08603.
- [65] H. B. Akins, C. M. Casey, N. Allen, M. B. Bagley, M. Dickinson, S. L. Finkelstein, M. Franco, S. Harish, P. Arrabal Haro, O. Ilbert, et al., *Astrophys. J.* **956**, 61 (2023), 2304.12347.
- [66] A. Sacchi and A. Bogdan, arXiv e-prints arXiv:2505.09669 (2025), 2505.09669.
- [67] Y. Ma, J. E. Greene, D. J. Setton, A. D. Goulding, M. Annunziatella, X. Fan, V. Kokorev, I. Labbe, J. Li, X. Lin, et al., arXiv e-prints arXiv:2504.08032 (2025), 2504.08032.
- [68] F. Pacucci and A. Loeb, arXiv e-prints arXiv:2506.03244 (2025), 2506.03244.
- [69] R. A. Daly, *Mon. Not. R. Astron. Soc.* **500**, 215 (2021), 2010.06908.